Tectonostratigraphy and provenance analysis to define the edge and evolution of the eastern Wuyi-Yunkai orogen, South China

WEIHUA YAO* & ZHENG-XIANG LI

Earth Dynamics Research Group, ARC Centre of Excellence for Core to Crust Fluid Systems (CCFS) and The Institute for Geoscience Research (TIGeR), Department of Applied Geology, Curtin University, Perth 6845, Australia

Abstract – We report three Palaeozoic sedimentary successions in northeastern South China that display markedly different tectonostratigraphic characteristics: the Jiangshan section exhibits an angular unconformity between the Upper Ordovician and Carboniferous stratra; the Shuangming section exhibits a disconformity between the lower Silurian and Upper Devonian strata; and the Xinqiao section exhibits a disconformity between the upper Silurian and Upper Devonian strata. The Shuangming and Xinqiao sections are interpreted to represent the remnant Nanhua foreland basin, whereas the Jiangshan section is in the fold-and-thrust zone of the Wuyi-Yunkai orogen. The Lizhu-Changshan thrust fault in between is interpreted to be the frontal thrust and the boundary of the orogen. Detrital provenance analysis of the Ordovician–Devonian sandstones from the Shuangming and Xinqiao sections shows that the Ordovician–Silurian, mid- to late-orogenic sandstones contain dominantly 860–780 Ma zircon populations and subordinate 2.5 Ga, 1.89–1.78 Ga, 980–950 Ma, 630–540 Ma and 430 Ma populations, indicating nearby sources including the early Neoproterozoic Sibao orogen, inverted Neoproterozoic rift basins and related plutons, recycled Ediacaran–Cambrian strata and, increasing with time, exposed Cathaysia basement and minor syn- to late-orogenic plutonic intrusions. The Devonian post-orogenic sandstones exhibit a dominant 440 Ma population with minor 2.5 Ga, 1.89–1.78 Ga, 860–780 Ma and 630–540 Ma populations, suggesting a dominant contribution from now widely exposed, mid- to late-orogenic plutonic intrusions (with or without contributions from rare volcanism of similar ages) in a residual topographic high SE of the Lizhu-Changshan fault. This residual topographic high of the Wuyi-Yunkai orogen had completely perished by early Carboniferous time, *c.* 60 Myr after the end of the orogenic event.

Keywords: tectonostratigraphy, detrital provenance, Wuyi–Yunkai Orogen, South China

1. Introduction

A collisional orogen generally consists of a series of metamorphic complexes in the core belt and a single (or double), evolving fold-and-thrust belt(s) as the outer belt(s). Syn-orogenic granitic intrusions are generally found in both belts (e.g. Moores & Twiss, 1995). Foreland basins are generally little-deformed sedimentary accommodations located on either one or both sides of the orogen, receiving eroded detritus off the mountain belts. The evolving nature of an orogenic system suggests that the fold-and-thrust belt generally migrates towards the foreland area during the orogenesis, incorporating the orogen side of the foreland basin into the fold-and-thrust belt (e.g. DeCelles & Giles, 1996). Both the transient margin (i.e. the frontal thrust) of an orogen and the evolving geometry and geographic extent of the foreland basin can be overprinted by younger tectonic events, making it a challenging task to define the margin(s) of an old orogenic belt. The lower Palaeozoic Wuyi-Yunkai orogen in South China is one such orogen.

The Wuyi-Yunkai orogeny was an Ordovician–Silurian intraplate orogenic event, likely caused by the far-field stress of the collision of the South China Block with northeastern Gondwana (e.g. Li, 1998; Wang *et al.* 2010; Yao *et al.* 2014; Yao & Li, 2016). This orogeny produced a series of early Palaeozoic metamorphic complexes along the Wuyi-Baiyun-Yunkai mountains (e.g. Wang *et al.* 2007; Yu *et al.* 2008; Li *et al.* 2010; Wan *et al.* 2010) that define the metamorphic orogenic core (Fig. 1a). The orogen shed sediments of thousands of metres thick in the evolving Nanhua foreland basin (Li, 1998; Yao & Li, 2016), and developed a large fold-and-thrust system to its NW. The Jiangshan-Shaoxing fault in northeastern South China (Fig. 1a) marks the boundary between the Yangtze and Cathaysia blocks (e.g. Zhao & Cawood, 1999; Li *et al.* 2002, 2009), but is probably largely a Phanerozoic feature formed after the amalgamation of the two blocks during early Neoproterozoic time (Li *et al.* 2002, 2009). Previous studies defined the Jiangshan-Shaoxing fault as the boundary between the orogenic core and fold-and-thrust zone when the Wuyi-Yunkai orogeny ceased by the end of the Silurian Period (e.g. Yao *et al.* 2012). However, due to strong Mesozoic tectonic modifications in the

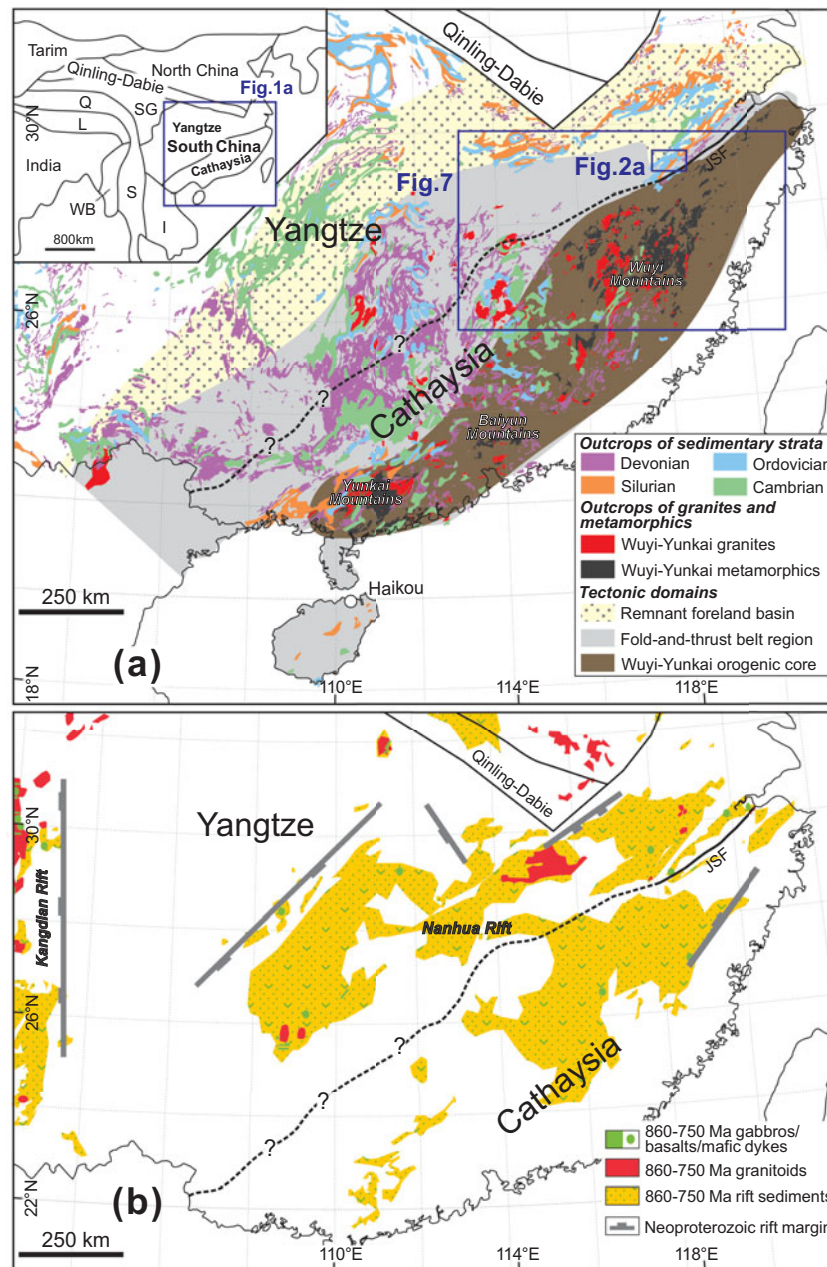*Author for correspondence: weihua.yao@curtin.edu.au

Figure 1. (Colour online) (a) A simplified regional map of the South China Block (SCB), highlighting the regional extent of the Ordovician–Silurian Wuyi-Yunkai orogenic core, fold-and-thrust belt and the remnant Nanhua foreland basin. Geological components such as distributions of Cambrian–Devonian sedimentary rocks, Wuyi-Yunkai syn-orogenic metamorphic rocks and granites are also presented in the map (after Yao & Li, 2016). The inset shows a sketch of major continental blocks/terranes in East Asia. (b) Distribution of mid-Neoproterozoic magmatic rocks (750–860 Ma) and continental rift sequences in South China (after Li et al. 2014). JSF – Jiangshan-Shaoxing Fault; L – Lhasa; Q – Qiangtang; SG – Songpan-Ganzi; WB – West Burma; S – Subumasu; I – Indochina.

region, neither the lateral extent of the Wuyi-Yunkai orogen nor the nature of the early Palaeozoic sedimentary dispersals in northeastern South China have been well constrained (e.g. Li *et al.* 2010; Xu *et al.* 2012).

Here we report the identification of the northern margin of an early Palaeozoic orogenic system in South China that was severely overprinted by Mesozoic orogenic and extensional events. We achieved this by analysing the varying tectonostratigraphic records along a traverse across the fold-and-thrust belt into the hinterland basin region. Together with a detrital provenance analysis of syn- and post-orogenic succes-

sions in the foreland basin, we construct the palaeogeographic evolution of the orogenic system.

2. Geological setting

The South China Block (SCB) consists of the Yangtze Block in the NW and the Cathaysia Block in the SE (Fig. 1a inset), which amalgamated during either 1140–880 Ma (e.g. Li *et al.* 2002, 2008, 2009; Greentree *et al.* 2006) or 870–820 Ma (e.g. Li, 1999; Zhao & Cawood, 1999; Wang *et al.* 2006, 2007; Wu *et al.* 2006). The middle Neoproterozoic Rodinia break-up

led to a massive production of *c.* 860–750 Ma bimodal magmatic rocks and deposition of rift sediments in both the southeastern South China Block (e.g. Li *et al.* 2003*a*, *b*; Li, Li & Li, 2005; Wang *et al.* 2006; Shu *et al.* 2011) and near the western Yangtze margin (e.g. Zhou *et al.* 2002, 2006; Li *et al.* 2003*a*) along the middle Neoproterozoic Kangdian Rift (Fig. 1b) (Li *et al.* 1999).

The first Phanerozoic tectonic event in the SCB after the Neoproterozoic rifting activities was the early Palaeozoic intraplate Wuyi-Yunkai orogeny, which led to the development of a prominent angular unconformity between upper Palaeozoic (Devonian and younger) and lower Palaeozoic (Silurian and/or older) sedimentary/meta-sedimentary rocks across southeastern South China (Huang *et al.* 1980; BGMRJX, 1984; BGMRGX, 1985; BGMRGD, 1988; BGMRHN, 1988; Ren, 1991; Wang *et al.* 2007; Li *et al.* 2010). This tectonic event was traditionally called the Caledonian orogeny (e.g. Ren, 1964, 1991; Huang *et al.* 1980; Yang, Cheng & Wang, 1986), but was renamed the Wuyi-Yunkai orogeny after the exposures of metamorphic orogenic core along the Wuyi, Baiyun and Yunkai mountains (Fig. 1a) (Li *et al.* 2010). The orogenic event began during Early Ordovician time and terminated during the Silurian Period (Yao & Li, 2016). By the end of Silurian time, the fully developed Wuyi-Yunkai orogen exhibited: (1) an orogenic core, defined by the distribution of 460–440 Ma high-grade metamorphic rocks; (2) a fold-and-thrust zone constrained by the extent of pre-Devonian deformation in the lower Palaeozoic strata as well as the distribution of 440–400 Ma granites; and (3) a remnant Nanhua foreland basin with non-deformed lower Palaeozoic sedimentary strata (Fig. 1a) (Li *et al.* 2014). The discovery of *c.* 435 Ma mafic igneous rocks in the Wuyi-Yunkai orogenic core (Yao *et al.* 2012; Wang *et al.* 2013) further helped to divide the Wuyi-Yunkai orogenic event into an Ordovician primary compression stage and a Silurian orogenic collapse stage (Li *et al.* 2010; Yao *et al.* 2012; Yao & Li, 2016).

Lower–middle Palaeozoic sedimentary rocks are well preserved in the northeastern corner of South China (Fig. 2a). Cambrian carbonates and cherts are deposited in a marine platform environment (BGMRZJ, 1989) and Ordovician–Silurian siliciclastics are deposited in a coastal marine to tidal environment, featured with fluidized sand veins and flame structures (Xu *et al.* 2012). Post-orogenic Devonian–Carboniferous delta to fluvial quartz-rich sediments were deposited on top of the Wuyi-Yunkai orogenic sequences, and their contact relationship varies across different localities (Fig. 3) (Li *et al.* 2014). The Wuyi-Yunkai fold-and-thrust belt features an angular unconformity between the Upper Ordovician and Carboniferous strata, whereas within the remnant Nanhua foreland basin there is a disconformity between the Silurian and Upper Devonian strata (Figs 2, 3). Representative tectonostratigraphic sections from the fold-and-thrust belt and the remnant foreland basin are se-

lected for detailed investigations in order to identify the lower Palaeozoic frontal thrust between them.

3. Tectonostratigraphic records

3.a. The Jiangshan section

The Jiangshan section, located in the Wuyi-Yunkai fold-and-thrust belt (Fig. 2b), is bounded by the Lizhu-Changshan thrust to the NW and the Jiangshan-Shaoxing fault to the SE (Fig. 2a). It comprises, from bottom to top, the Cambrian Hetang, Yangliugang, Huayansi and Xiyangshan formations, the Lower Ordovician Yinzhubu and Ningguo formations, the Middle Ordovician Hule and Niushang formations, and the Upper Ordovician Huangnigang and Changwu formations (Fig. 3) (RGMRZJ-a, 1966; BGMRZJ, 1989).

The Cambrian succession, including the Hetang, Yangliugang, Huayansi and Xiyangshan formations, is dominated by greyish and grey-blackish limestones, dolomitic limestones and thin-bedded dolomites (see Li *et al.* 2014, fig. 2.20) with chert interlayers at the bottom (RGMRZJ-a, 1966; BGMRZJ, 1989). The Cambrian age was constrained by the presence of trilobites *Paralisaniella* sp. and *Oidalagnostus* sp. found in the strata. The Ordovician Yinzhubu and Ningguo formations are composed mainly of calcareous muddy siltstones and mudstones, interstratified with minor thin black shale layers at the upper part and manganic nodules at the bottom, and host Early Ordovician graptolites *Didymograplus* sp. (RGMRZJ-a, 1966). The Ordovician Niushang and Hule formations are very thin (Fig. 3), consisting mainly of black shales and carbonates, and gradually transit into yellowish siltstones near the top (RGMRZJ-a, 1966; BGMRZJ, 1989). The age of the Niushang and Hule formations is defined by Middle Ordovician graptolites *Climacograptus* cf. and brachiopods *Shumardia* sp. (RGMRZJ-a, 1966). The Yanwashan Formation nodular limestones and the Huangnigang Formation calcareous nodule-bearing silty mudstones are of Late Ordovician age constrained by the cephalopods *Michelinoceras* sp. and trilobites *Nankinolithus nankinensis* (BGMRZJ, 1989). The Changwu Formation consists mainly of yellowish siltstones and fine-grained sandstones interlayered with calcareous mudstones (Fig. 3). It contains Late Ordovician brachiopods *Rafinesquaina* sp. and *Sowerbyella* sp. and graptolites *Orthograptus* sp. (BGMRZJ, 1989).

The pebbly quartz sandstone layers of the lower Carboniferous Yejiatang Formation sit above the Ordovician Changwu Formation with an angular unconformity (Fig. 3; also see Li *et al.* 2014, fig. 2.22c of), leaving an uppermost Ordovician – Devonian hiatus in the Jiangshan section (RGMRZJ-a, 1966; BGMRZJ, 1989; Rong *et al.* 2010).

3.b. The Shuangming section

The Shuangming section, located in the remnant Nanhua foreland basin (Fig. 2b), is bounded by the
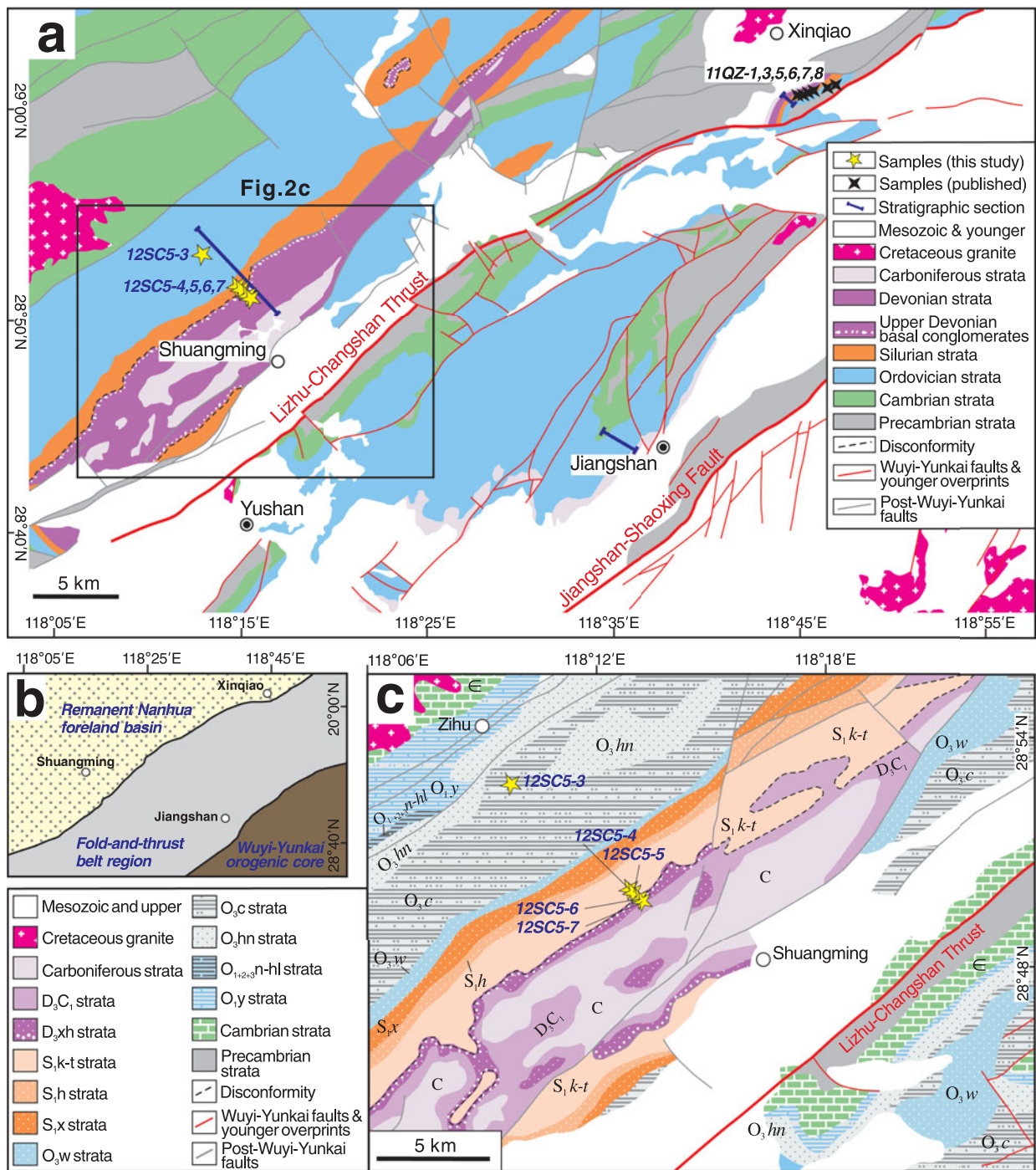
Figure 2. (Colour online) (a) Geological map of the Jiangshan-Shuangming-Xinqiao region and geological traverses for stratigraphic logging and sampling (after RGMRZJ-b, 1970; Li *et al.* 2014). (b) A simplified map of (a), showing the three tectonics domains and relevant locations of the Jiangshan, Shuangming and Xinqiao sections. (c) Enlarged geological map of the Shuangming region NW of the Lizhu-Changshan thrust fault (after RGMRZJ-b, 1970; Li *et al.* 2014), highlighting sampling locations and the Cambrian–Devonian stratigraphic formations.

Lizhu-Changshan thrust to the SE (Fig. 2a). It comprises a continuous Cambrian – lower Silurian succession conformably overlain by an Upper Devonian succession (Figs 2, 3) (BGMRZJ, 1989; RGMRZJ-b, 1970). The Cambrian strata consist of the Hetang, Dachengling, Yangliugang, Huayansi and Xiyangshan formations, all dominantly carbonates and dolomites with black carbonaceous cherts at the bottom (RGMRZJ-b, 1970; BGMRZJ, 1989). The Lower

Ordovician Yinzhubu Formation consists mainly of calcareous mudstones with minor limestone nodules and siltstones, and some banded limestones near the bottom of the formation (see Li *et al.* 2014, fig. 2.25a). Early Ordovician graptolites *Didymograplus* sp. are found in the Yinzhubu Formation, making it correlatable to the Jiangshan Yinzhubu Formation (RGMRZJ-b, 1970; BGMRZJ, 1989). The Ordovician Ningguo-Hule Formation consists of black
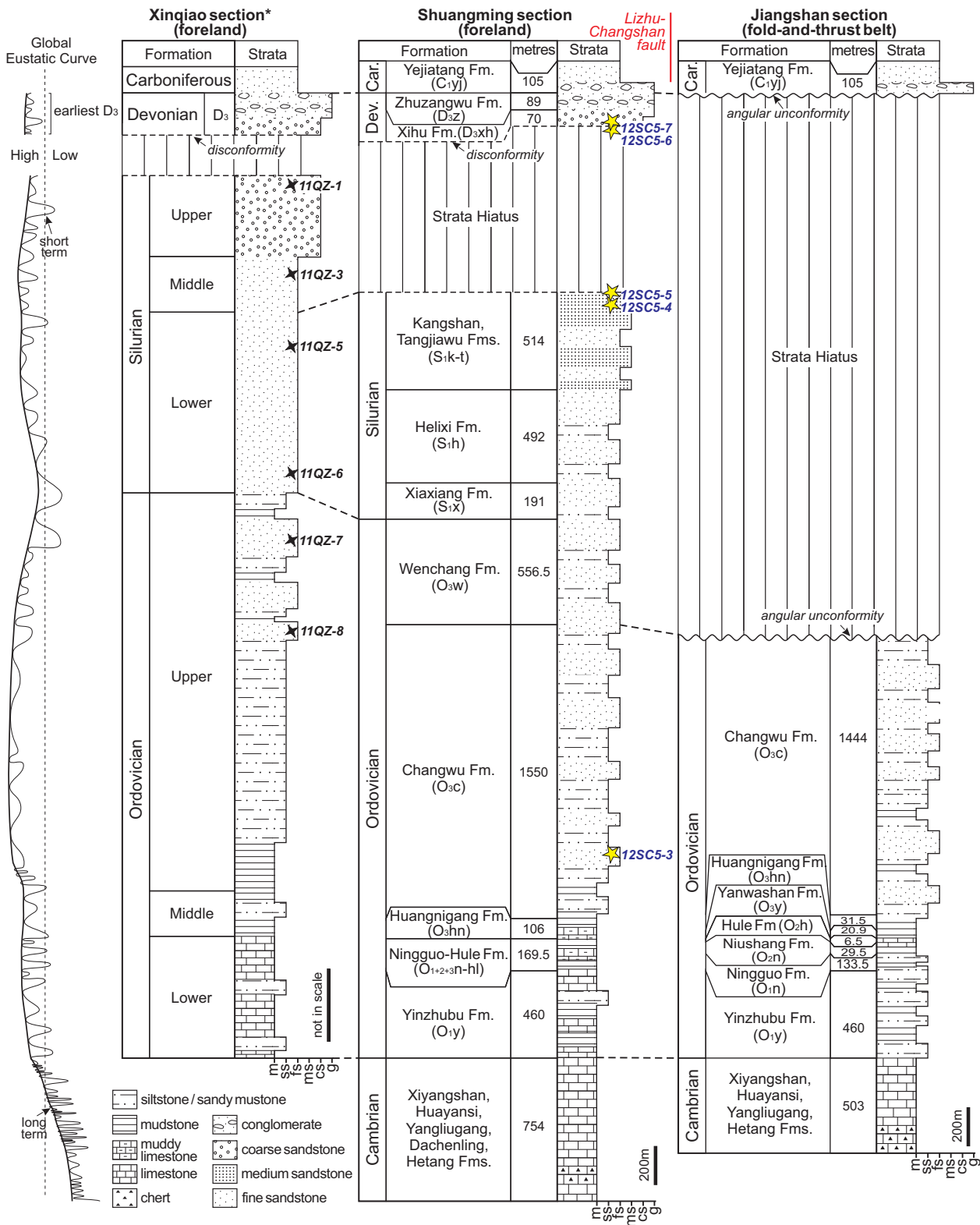
Figure 3. (Colour online) Generalized Cambrian–Devonian tectonostratigraphic columns of the Xinqiao and Shuangming sections from the remnant Nanhua foreland basin and the Jiangshan section from the Wuyi-Yunkai fold-and-thrust belt. The thickness of each stratigraphic formation in the Shuangming and Jiangshan sections is marked in metres, and siliciclastic samples for provenance analysis are marked against the columns. The long-term and short-term global eustatic curves are from Haq & Schutter (2008). The asterisk-marked Xinqiao section is adopted from Xu *et al.* (2012). Lithological abbreviations: m – mudstone/shale; ss – siltstone; fs – fine-grained sandstone; ms – medium-grained sandstone; cs – coarse-grained sandstone; g – gravel/conglomerate.

Table 1. Summary of Palaeozoic siliciclastic samples from the Shuangming and Xinqiao sections, NE South China

Samples	Coordinates (N, E)	Stratigraphic age	Lithology
Shuangming section (this study)			
12SC05-7	28° 49′ 38.6″, 18° 12′ 57.2″	Upper Devonian	Pebbly coarse-grained sandstone
12SC05-6	28° 49′ 40.0″, 18° 12′ 56.6″	Upper Devonian	Greyish coarse-grained quartz sandstone
12SC05-5	28° 49′ 44.1″, 18° 12′ 53.3″	Lower Silurian	Pinkish medium-grained sandstone
12SC05-4	28° 49′ 45.8″, 18° 12′ 51.9″	Lower Silurian	Pinkish medium-grained sandstone
12SC05-3	28° 52′ 45.7″, 18° 09′ 35.4″	Upper Ordovician	Greyish fine-grained sandstone
Xingqiao section (Xu *et al.* 2012)			
11QZ-1	NA	Upper Silurian	Pale-green coarse-grained sandstone
11QZ-3	NA	Middle Silurian	Pale-green medium-grained sandstone
11QZ-5	NA	Lower Silurian	Grey medium-grained sandstone
11QZ-6	NA	Lower Silurian	Grey medium-grained sandstone
11QZ-7	NA	Upper Ordovician	Grey fine-grained sandstone
11QZ-8	NA	Upper Ordovician	Grey silty mudstone

NA – not applicable.

carbonaceous shales interlayered with minor nodular muddy limestones (see Li *et al.* 2014, fig. 2.25c). The Upper Ordovician Huangnigang Formation, featuring abundant limestone nodules in calcareous mudstones, hosts Late Ordovician trilobites *Hammatocnemis*, *Paraphilipsinella* and *Sarkia* (RGMRZJ-b, 1970). The Upper Ordovician Changwu and Wenchang formations are extremely thick (up to *c.* 2100 m in total; Fig. 3), consisting mainly of greyish siltstones and fine-grained sandstones with minor mudstone interlayers (BGMRZJ, 1989). Late Ordovician trilobites *Hammatocnemis*, *Telephima* and *Amphitrion* are present in these two formations (RGMRZJ-b, 1970; BGMRZJ, 1989). Sedimentary structures such as micro-ripples have been found in the Changwu Formation (see Li *et al.* 2014, fig. 2.26a). The overlying Xiaxiang, Helixi, Kangshan and Tangjiawu formations, defined as being of lower Silurian age by fossils *Eupoikilofusa* sp. and *Trachysphaeridium* sp. in the strata (BGMRZJ, 1989), are composed of yellowish and greenish siltstones, fine-grained sandstones and medium-grained quartz sandstones. Both the grain size and the percentage of siliciclastics increase upwards (RGMRZJ-b, 1970).

Disconformably overlying the lower Silurian strata are the Upper Devonian Xihu and Zhuzangwu formations, consisting of greyish coarse-grained quartz sandstones and pebbly sandstones (Fig. 3). They host Devonian fossils *Plagiozamites oblongifolius* and *Platyphyllum ginkgophylloides* (BGMRZJ, 1989; Rong *et al.* 2010). The Zhuzangwu Formation is in turn conformably overlain by the lower Carboniferous Yejiatang Formation siliciclastic strata (Fig. 3) (RGMRZJ-b, 1970).

Along the Shuangming section we collected a fine-grained sandstone sample from the Upper Ordovician Changwu Formation, two medium-grained sandstone samples from the lower Silurian Kangshan and Tangjiawu formations right beneath the disconformity, and two coarse-grained quartz sandstone samples from the Upper Devonian Xihu Formation above the disconformity for detrital provenance analysis (Fig. 3). Table 1 summarizes the general information regarding the sampled siliciclastic sedimentary rocks from the region.

4. Analytical procedures for provenance analysis

4.a. Sample preparation

Zircon crystals were extracted from bulk rocks using standard density and magnetic separation techniques at the Hebei Regional Geology and Mineral Survey in Langfang. Zircon grains, together with zircon U–Pb standard 91500 and Plešovice were cast in epoxy mounts and then polished to section the crystal in half for analyses. All analysed zircon grains were imaged in transmitted and reflected light as well as cathodoluminescence (CL) light at Curtin University, Australia, to better reveal the internal structures of the grains.

4.b. Zircon U–Pb geochronology

U–Th–Pb concentrations were measured using the laser ablation inductively coupled plasma mass spectrometry (LA-ICP-MS) facility at the Institute of Geology and Geophysics, Chinese Academy of Sciences (IGG-CAS). External zircon standards 91500 with $^{207}U/^{206}Pb$ age of 1065.4 ± 0.6 Ma (Wiedenbeck *et al.*, 1995, 2004) and GJ-1 with $^{206}U/^{238}Pb$ age of 608.5 ± 0.4 Ma (Jackson *et al.* 2004) were employed to calibrate U–Th–Pb ratios of unknown zircon grains. Glass NIST 610 was used for Th/U ratio determination. The ablation pits on zircon grains were *c.* 36 μm in diameter and 20–30 μm in depth, and the detailed analytical procedure followed that of Xie *et al.* (2008). Data reduction was carried out using Glitter v4.0 (Van Achterbergh *et al.* 2001), ComPbCorr#3_151 (Anderson, 2002) and Isoplot/Ex v2.49 (Ludwig, 2001) packages. Zircon U–Pb data of all five analysed samples are provided in online Supplementary Table S1 (available at http://journals.cambridge.org/geo), in which the analyses with discordance >10 % are formatted in italics.

4.c. Zircon Hf isotopic analysis

Laser ablation zircon Lu–Hf isotopic analyses were conducted at IGG-CAS using a ThermoFinnigan Neptune multicollector (MC-) ICP-MS equipped with a 193 nm laser. Zircon 91500 and GJ-1 were used as

reference standards, with a recommended $^{176}Hf/^{177}Hf$ ratio of 0.282307 ± 0.000031 (2σ) (Wu *et al.* 2006) and 0.282000 ± 0.000005 (2σ) (Morel *et al.* 2008), respectively. Laser ablation Hf sites were centred as close as possible to the spots for U–Pb dating, with spot sizes of *c.* 60 µm in diameter and *c.* 45 µm in depth. More details on analytical and calibration procedures can be found in Wu *et al.* (2006). A decay constant for ^{176}Lu of $1.867 \pm 0.008 \times 10^{-11}$ a^{-1} (Soderlund *et al.* 2004), the present-day chondritic ratios of $^{176}Hf/^{177}Hf = 0.282772$ and $^{176}Lu/^{177}Hf = 0.0332$ (Blichert-Toft & Albarede, 1997) were accepted for calculating $\varepsilon_{Hf}(t)$ values. One-stage model ages (T_{DM}) were calculated relative to depleted mantle with a present-day $(^{176}Hf/^{177}Hf)_{DM}$ of 0.28325 and $(^{176}Lu/^{177}Hf)_{DM}$ of 0.0384 (Griffin *et al.* 2000). Two-stage model ages $(T_{DM}{}^C)$ were calculated by forcing a growth curve through the zircon initial ratio with assumed $(^{176}Lu/^{177}Hf)_C$ values of 0.0093 and 0.015, corresponding to the Proterozoic upper continental crust (Amelin *et al.* 1999) and Phanerozoic upper continental crust (Griffin *et al.* 2000), respectively. Zircon Lu–Hf isotopic data of all five analysed samples are presented in online Supplementary Table S2 (available at http://journals.cambridge.org/geo).

5. Results of provenance analysis

5.a. Zircon U–Pb ages

One Upper Ordovician greyish-green, fine-grained sandstone sample (12SC05-3) from the Changwu Formation (Fig. 3) was collected from the Shuangming section for detrital provenance analysis (Table 1). Seventy concordant U–Pb ages were obtained from 70 single zircon grains, ranging from 445 Ma to 2800 Ma (Fig. 4a). A predominant age peak of 780 Ma (28 % of all analyses) and a subordinate age population of 750 Ma (17 % of all analyses) are present, whereas the remaining ages are evenly distributed between 445–630 Ma and 920–2800 Ma (Fig. 5a). One single grain among the 70 analyses gives a $^{206}Pb/^{238}U$ age of 445 ± 5 Ma for the sample, which is much younger than the youngest age cluster of 630 Ma (Fig. 4a). The age of 445 ± 5 Ma from this single grain, indicating a potential maximum depositional age, is consistent within error with the Late Ordovician biostratigraphic age assigned for the Changwu Formation. More such analyses are required to provide a more robust maximum depositional age.

Samples 12SC05-4 and 12SC05-5 are pinkish medium-grained sandstone samples from the lower Silurian Kangshan and Tangjiawu formations of the Shuangming section (Fig. 3; Table 1). Eighty U–Pb analyses on 80 zircon grains were conducted for each sample, all of which yielded concordant ages (Fig. 4b, c). Ages for sample 12SC05-4 range from 435 Ma to 2800 Ma (Fig. 4b), with a major age population of 785 Ma and moderate populations of 450 Ma, 540 Ma and 2450 Ma (Fig. 5b). Sample 12SC05-5 yielded pre-

vailing age peaks of 775 Ma and 820 Ma, with subordinate peaks of 435 Ma, 1950 Ma and 2450 Ma (Fig. 5c). The 'Pan-African' ages of 540–630 Ma also left imprints on these two samples. The youngest age group of sample 12SC05-4 (three analyses) gives a weighted mean $^{206}Pb/^{238}U$ age of 436 ± 11 Ma ($n = 3$, MSWD = 2.3, Fig. 4b), indicating a maximum depositional age of *c.* 435 Ma. The four youngest analyses of sample 12SC05-5 yield a weighted mean $^{206}Pb/^{238}U$ age of 434 ± 10 Ma ($n = 4$, MSWD = 1.3, Fig. 4c), implying a maximum depositional age of *c.* 435 Ma which is consistent with the middle Silurian biostratigraphic age.

Samples 12SC05-6 and 12SC05-7 are collected from the Upper Devonian Xihu Formation in the Shuangming section, which overlies the lower Silurian strata with a disconformable contact (Fig. 3). Sample 12SC05-6 is a greyish coarse-grained quartz sandstone (Table 1), in which 70 concordant U–Pb ages were obtained from 80 analyses on 80 individual zircon grains (Fig. 4d). The concordant ages range from 388 Ma to 2600 Ma, yielding a dominant cluster at 442 Ma (39 % of all analyses), and minor 580–680 Ma (Pan-African) and 800–890 Ma Neoproterozoic populations (Fig. 5d). Proterozoic ages older than 1200 Ma count for 20 % of all analyses (Fig. 4d). The youngest six concordant analyses of samples 12SC05-6 yield a weighted mean $^{206}Pb/^{238}U$ age of 397 ± 10 Ma ($n = 6$, MSWD = 2.3, Fig. 4d), implying a maximum depositional age of *c.* 400 Ma. Sample 12SC05-7 is a pebbly coarse-grained quartz sandstone (Table 1), for which 74 concordant U–Pb ages were obtained from 80 analyses on 80 individual zircon grains (Fig. 4e). The concordant ages range from 410 Ma to 2660 Ma, and form a dominant cluster of 445 Ma (45 % of all analyses, Fig. 5e). This sample also yields subordinate Neoproterozoic populations of age 775–875 Ma and a few Proterozoic ages (Fig. 5e). The youngest six concordant analyses of samples 12SC05-7 yield a weighted mean $^{206}Pb/^{238}U$ age of 413 ± 20 Ma ($n = 6$, MSWD = 0.01, Fig. 4e), implying a maximum depositional age of *c.* 400 Ma within error, consistent with that of sample 12SC05-6.

5.b. Zircon Hf isotopes

A total of 228 detrital zircons from the three mid- to late-orogenic samples (12SC05-3, 12SC05-4 and 12SC05-5) from the Shuangming section (Figs 2, 3) which gave concordant U–Pb ages were selected for *in situ* Hf isotopic analysis. The analysed zircons yielded highly variable $^{176}Hf/^{177}Hf$ ratios (0.280492–0.282688) and $\varepsilon_{Hf}(t)$ values (−27.6 to 12.0) (online Supplementary Table S2, available at http://journals.cambridge.org/geo). Three grains plot above the new continental crust line; the remaining 223 zircons plot on or below the line, with 78 % of them yielding negative $\varepsilon_{Hf}(t)$ values (Fig. 6).

In situ zircon Hf isotopic analysis was also conducted on 62 detrital zircons with concordant U–Pb ages
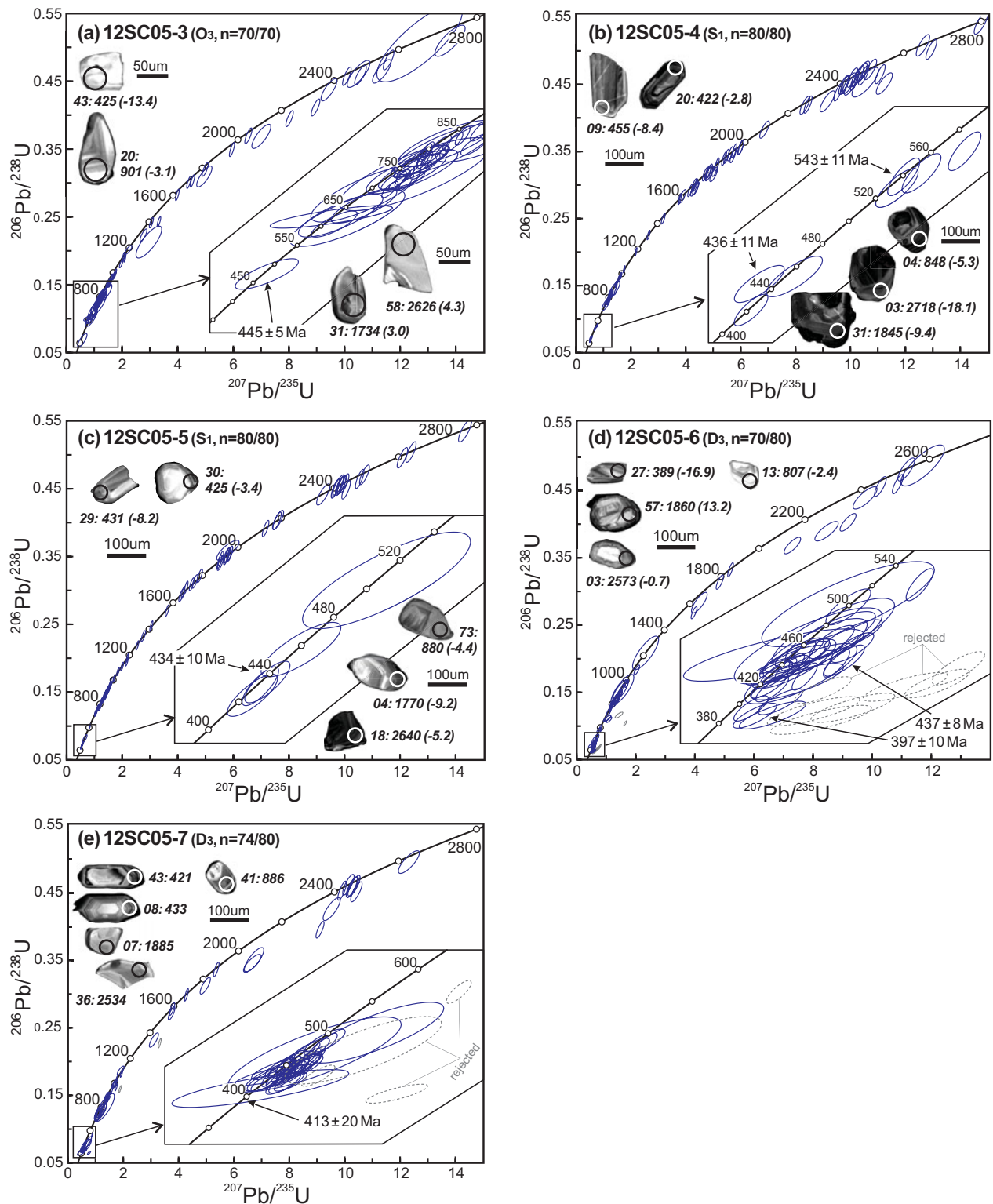
Figure 4. (Colour online) (a–e) Zircon U–Pb Concordia plots and CL images of the Ordovician–Devonian sandstone samples from the Shuangming section. Number of concordant analyses/total number of analyses is denoted *n* and the concordance is within 90–110 % for this study. Analytical spots, ages and $\varepsilon_{Hf}(t)$ values are formatted in italics next to corresponding CL images of the zircon grains, e.g. *43: 425 (–13.4)* represents spot number 43 with an age of 425 Ma and $\varepsilon_{Hf}(t)$ value of –13.4 for sample 12SC05-3.

from the post-orogenic sample 12SC05-6 (Figs 2, 3). The results again display highly variable $^{176}Hf/^{177}Hf$ ratios (0.280919–0.282515) and $\varepsilon_{Hf}(t)$ values (−48.2 to 13.2) (online Supplementary Table S2). Apart from one zircon grain with an age of 1860 Ma, all others

plot on or below the new continental crust line (Fig. 6). Notably, all *c.* 440 Ma zircons plot below the chondritic uniform reservoir line with negative $\varepsilon_{Hf}(t)$ values, consistent with that of the majority of syn-orogenic magmatic zircons (Fig. 6).
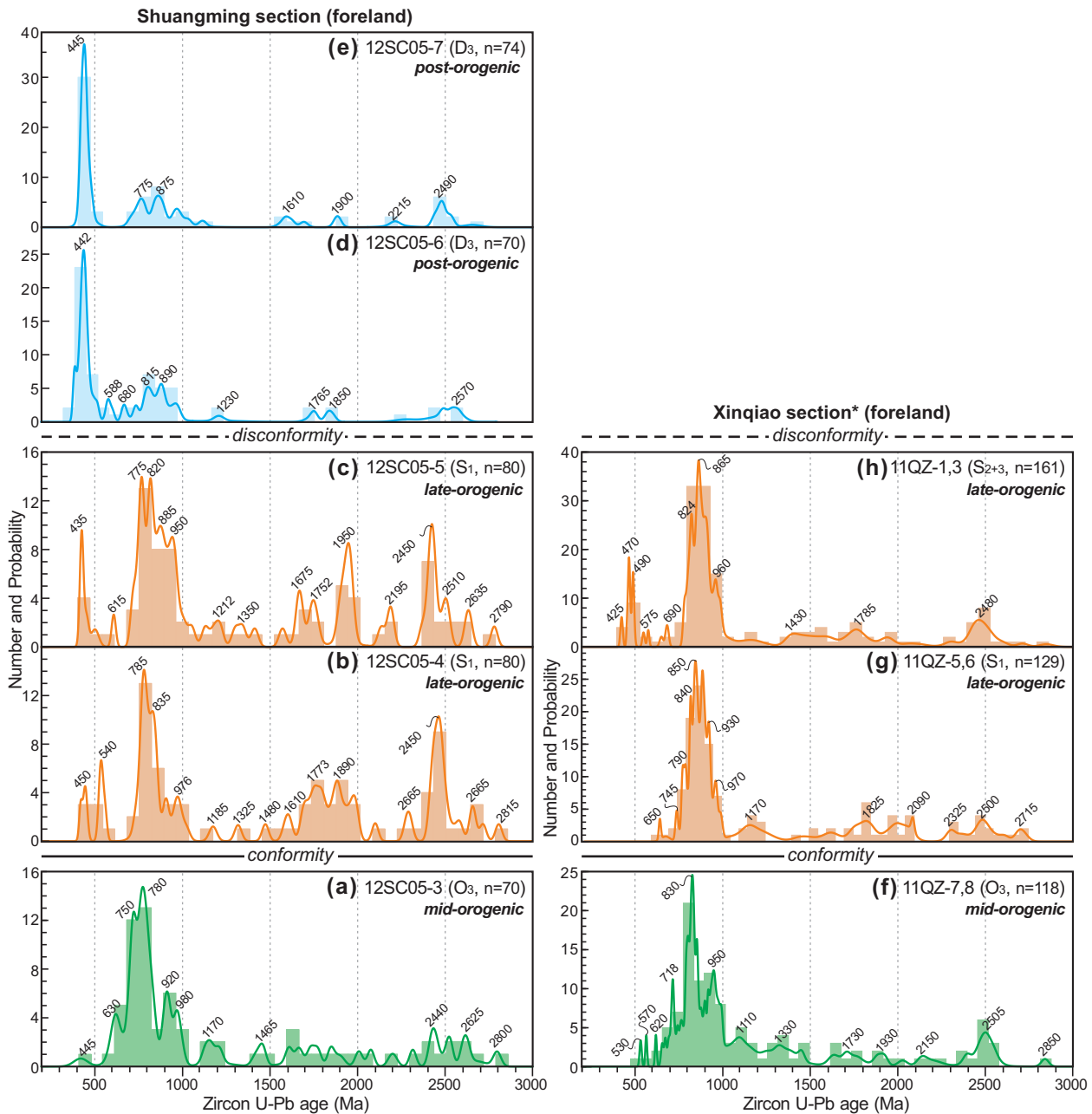
Figure 5. (Colour online) Relative probability and density histogram plots of zircon U–Pb ages with 90–110 % concordance of (a) mid-orogenic Upper Ordovician sample 12SC05-3; (b) late-orogenic Lower Silurian sample 12SC05-4; (c) late-orogenic Lower Silurian sample 12SC05-5; (d) post-orogenic Upper Devonian sample 12SC05-6; (e) post-orogenic Upper Devonian sample 12SC05-7 from the Shuangming section; (f) mid-orogenic Upper Ordovician samples; (g) late-orogenic Lower Silurian samples; and (h) late-orogenic Middle–Upper Silurian samples from the Xinqiao section. The Xinqiao samples are from Xu *et al.* (2012).

6. Discussion

6.a. Contrasting tectonostratigraphic records define the northern boundary of the Wuyi-Yunkai orogen

Lower Palaeozoic stratigraphy in northeastern South China generally reflects a coarsening upwards trend. Sedimentary facies evolve from: shallow-marine carbonate platform in the Cambrian deposits; to a neritic estuary/lagoon in the Lower–Middle Ordovician stratigraphy where interlayered nodular carbonates, mudstones and siltstones were deposited; to finally delta to tidal flat in Upper Ordovician – Silurian strata with increasing terrestrial deposits (BGMRZJ,

1989; Rong *et al.* 2010; Xu *et al.* 2012). The early Palaeozoic eustatic curves (Haq & Schutter, 2008) indicate a long-term global sea-level rise during Cambrian – Middle Ordovician time, predicting an upwards-fining sedimentary package. However, the Cambrian – Middle Ordovician sequences observed in the Shuangming and Jiangshan sections show upwards grain-coarsening and siliciclastic-increasing trends (Fig. 3), indicating that the onset of the Wuyi-Yunkai orogeny likely dominated the local sedimentation in a foreland basin environment (Li *et al.* 2014; Yao & Li, 2016). The global sea level fluctuated with a slight sea-level lowering during Late Ordovician
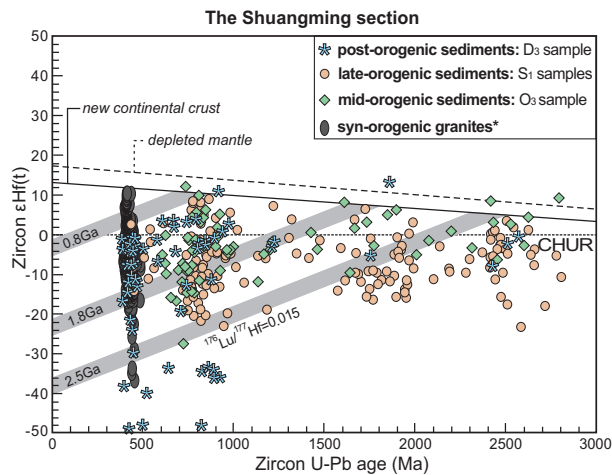
Figure 6. (Colour online) Zircon $\varepsilon_{Hf}(t)$ values versus U–Pb ages plot for the mid-orogenic Upper Ordovician samples, late-orogenic Silurian samples and post-orogenic Upper Devonian samples. Zircon Hf values of syn-orogenic magmatic zircons from early Palaeozoic granites across the entire Wuyi-Yunkai orogen (Yu *et al.* 2016) are plotted for comparison. The depleted mantle and new continental crust evolution lines were extrapolated after Griffin *et al.* (2000) and Dhuime, Hawkesworth & Cawood (2011), respectively. Potential crustal evolution lines at 2.5 Ga, 1.8 Ga and 0.8 Ga are calculated for the average continental crust of $^{176}Lu/^{177}Hf$ value of 0.015 (Griffin *et al.* 2000).

time (Haq & Schutter, 2008), coinciding with the upwards-coarsening siliciclastic sedimentation in all three stratigraphic sections of the study region (Fig. 3). However, during Silurian time, the general trend of global sea-level rise again contradicted the upwards-coarsening Silurian packages in the region (Fig. 3) (RGMRZJ-a, 1966; RGMRZJ-b, 1970; BG-MRZJ, 1989), indicating that local tectonics likely still dominated the basin evolution.

The Jiangshan section within the Wuyi-Yunkai fold-and-thrust belt (Fig. 2b) features an earlier sedimentary transition from Cambrian marine carbonates to Ordovician shallow-water siliciclastics in comparison to the other sections, as well as an angular unconformity between the Ordovician strata and the lower Carboniferous strata (Figs 2, 3). The Wuyi-Yunkai orogeny started by Early Ordovician time (*c.* 490–480 Ma), featuring continental uplift along the southeastern coastal Cathaysia (Liu & Xu 1994; Yao & Li, 2016). By Late Ordovician time, the uplifted orogen expanded to a >150 km wide zone along the present-day coastal Cathaysia, but was still distant from the Jiangshan section (Fig. 7a). The study region, including the Jiangshan, Shuangming and Xinqiao sections, was still receiving fine siliciclastic sedimentation with supplies from the SE during that time.

By early Silurian time, the uplifted orogen propagated further towards the NW hinterland, covering most of the Cathaysia Block. With the Jiangshan-Shaoxing thrust likely starting to form just west of it, the study region started to receive sediments more proximal to the orogenic front. Although no strata of early Silurian age have been preserved in the Jiangshan section

(Fig. 3), elsewhere in this structural zone early Silurian conglomeratic lithofacies have been preserved. In contrast, the Shuangming and Xinqiao sections further to the NW received early Silurian sandy deposition (Fig. 7b).

Tectono-magmatic analyses and petrological studies indicate that the Wuyi-Yunkai orogen experienced orogenic root delamination no later than early Silurian time (*c.* 435 Ma, Li *et al.* 2010; Yao *et al.* 2012). As a consequence, the orogenic belt was expected to experience a phase of topographic uplift due to isostatic rebound following that event, and possibly a phase of orogenic collapse (Li *et al.* 2010; Yao *et al.* 2012; Yao & Li, 2016). Regardless of whether the orogen continued with compression or entered a collapse stage during Silurian time, the orogen appeared to have expanded further to the NW during this period. The Jiangshan section likely became a topographic high during this stage (Fig. 7c) with no late Silurian deposition preserved there, and older strata likely experienced erosion. In contrast, the Xinqiao section remained in a subaerial environment not far from the Jiangshan topographic high, receiving coarser-grained, proximal siliciclastics deposition (Figs 3, 7c) (BGMRZJ, 1989; Rong *et al.* 2010).

Following a widespread late Silurian – Early Devonian peneplanation, South China underwent a marine transgression from its SW corner during Devonian time (Liu & Xu, 1994). The Shuangming and Xinqiao sections received Upper Devonian fluvial to nearshore, quartz-rich basal conglomerate and pebbly sandstones, whereas the Jiangshan section remained at an elevated palaeotopography throughout the Devonian Period (residual topography of the Wuyi-Yunkai orogen) (Figs 3, 7d).

We therefore observe two contrasting stratigraphic contact relationships on the two sides of the Lizhu-Changshan thrust (Figs 2, 3): an angular unconformity between the Upper Ordovician and lower Carboniferous strata in the Jiangshan section to its SE (Fig. 3); and a disconformity between Silurian and Devonian strata to its NW. The angular unconformity to its SE corresponds to the widespread angular unconformity between the upper Palaeozoic terrestrial and marine deposits (Devonian and younger) and the variably deformed and metamorphosed lower Palaeozoic successions (Silurian and older) over much of southeastern South China (e.g. Huang *et al.* 1980; Ren, 1991; Charvet *et al.* 2010; Li *et al.* 2010), which defines the lateral extent of the Wuyi-Yunkai orogen (including its fold-and-thrust belt). On the contrary, disconformities between the Silurian and Upper Devonian strata to the NW of the Lizhu-Changshan thrust (Figs 2, 3) indicate that this region was the remnant Nanhua foreland basin at the end of the Wuyi-Yunkai orogeny, which experienced no early Palaeozoic deformation. Based on this contrasting tectonostratigraphic observation, we interpret the Lizhu-Changshan thrust (Fig. 2a) to be the northwestern terminal frontal thrust of the Wuyi-Yunkai fold-and-thrust belt, defining the northwestern
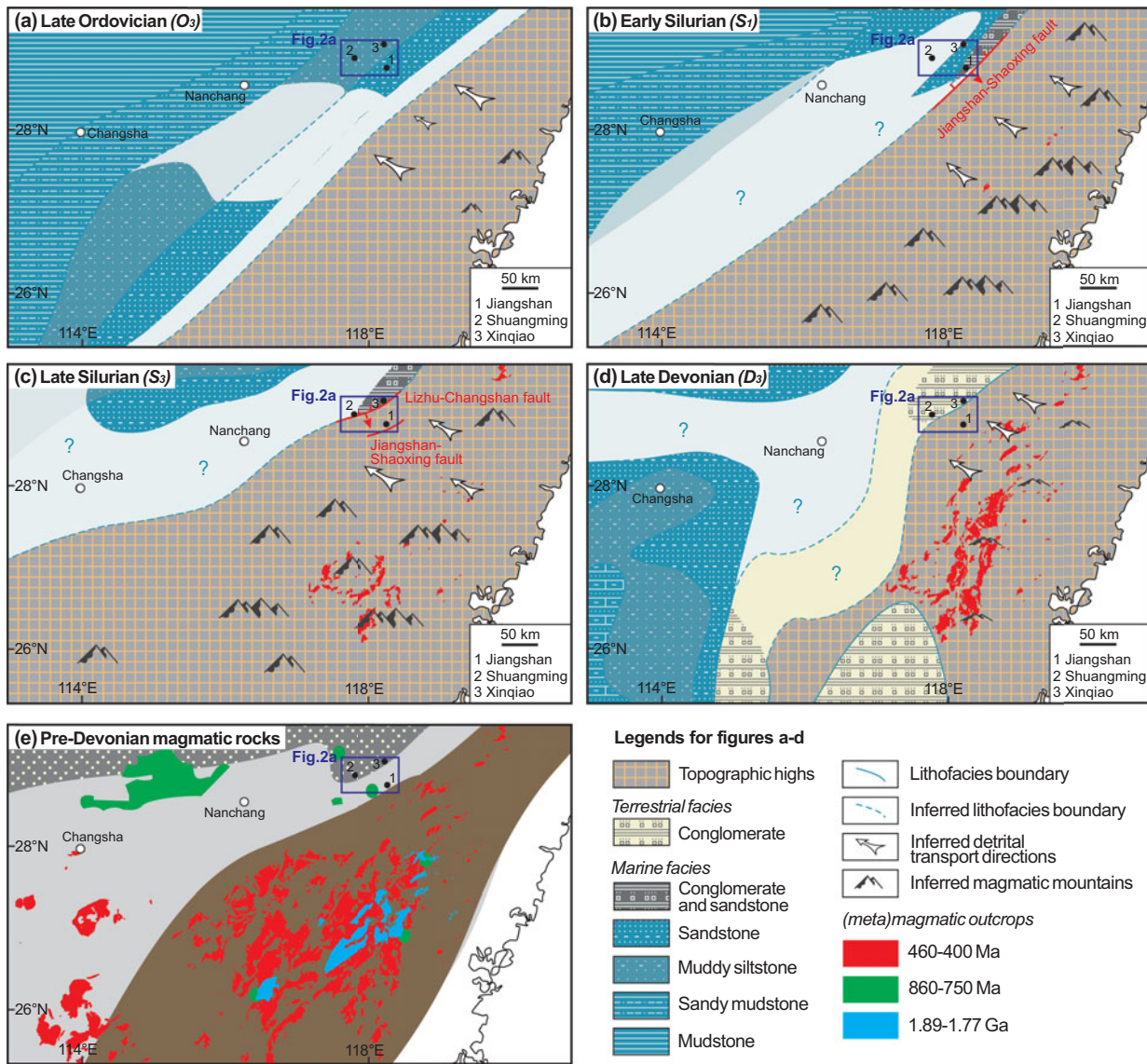
Figure 7. (Colour online) Palaeogeographic maps of northeastern South China covering the Xinqiao, Shuangming and Jiangshan sections and surrounding areas during the time intervals: (a) Late Ordovician; (b) early Silurian; (c) late Silurian; and (d) Late Devonian (after Liu & Xu, 1994; Yao *et al*. 2015). (e) Distribution of 1.77–1.89 Ga crystalline basement rocks, and 750–860 Ma and 400–460 Ma (meta)magmatic rocks in northeastern South China.

margin of the much reworked early Palaeozoic orogen (Fig. 1a).

6.b. Detectable provenance changes defining the evolving Wuyi-Yunkai orogen

Figure 1a shows the terminating stage of the Wuyi-Yunkai orogen (including both the fold-and-thrust belt and the orogenic core) and the remnant Nanhua foreland basin towards the end of Silurian time. Due to the evolving nature of the orogen–basin system, the Nanhua foreland basin recorded dramatic changes in the detritus shed off from the Wuyi-Yunkai orogen through time. By tracking such provenance changes through time we could better define how the Wuyi-Yunkai orogen evolved.

Our provenance analysis utilizes new data from sandstone samples both below and above the discon-

formity in the Shuangming section (Figs 3, 5), supplemented by published data from six Ordovician–Silurian samples from the Xinqiao section (Fig. 3) (Xu *et al*. 2012). The Shuangming samples can be grouped into three categories based on their U–Pb age patterns and chronostratigraphic natures: (1) the mid-orogenic group (Late Ordovician) that features a predominant *c.* 780 Ma age population with negligible Palaeozoic signature (Fig. 5a); (2) the late-orogenic group (early Silurian) that features a *c.* 780 Ma age population and increasing 435–540 Ma age peaks, and Archaean–Palaeoproterozoic basement signals (Fig. 5b, c); and (3) the post-orogenic group (Late Devonian) that shows an overwhelming *c.* 440 Ma age peak and suppressed Neoproterozoic and older basement age populations (Fig. 5d, e). The Xinqiao samples (Xu *et al*. 2012) can be similarly divided into two groups: (1) the mid-orogenic group (Late Ordovician) that features a

Table 2. *Two-sample Kolmogorov–Smirnov (K-S) test on the Ordovician–Devonian samples from the Shuangming section. The results reflect the input of both determined ages and errors for each zircon grain. Probability (P value) > 0.05 (in bold) indicates that the compared pair of samples cannot be statistically distinguished at 95 % confidence level. The software (K-S test 1.0.xls) used in this study is from the University of Arizona, USA.*

D value / P value	12SC05-3	12SC05-4	12SC05-5	12SC05-6	12SC05-7
12SC05-3	–	0.255	0.194	0.457	0.429
12SC05-4	**0.106**	–	0.136	0.441	0.401
12SC05-5	**0.117**	**0.452**	–	0.451	0.383
12SC05-6	0.000	0.000	0.000	–	0.074
12SC05-7	0.000	0.000	0.000	**0.989**	–

Table 3. *Two-sample Kolmogorov–Smirnov (K-S) test on the Ordovician–Devonian samples from the Xinqiao section (Xu et al. 2012).*

D value / P value	11QZ-1	11QZ-3	11QZ-5	11QZ-6	11QZ-7	11QZ-8
11QZ-1	–	0.206	0.159	0.096	0.179	0.115
11QZ-3	**0.067**	–	0.113	0.199	0.092	0.321
11QZ-5	**0.369**	**0.737**	–	0.170	0.129	0.269
11QZ-6	**0.905**	**0.100**	**0.310**	–	0.229	0.123
11QZ-7	**0.214**	**0.903**	**0.654**	**0.060**	–	0.240
11QZ-8	**0.824**	**0.103**	**0.134**	**0.769**	**0.072**	–

Table 4. *Combined Shuangming–Xinqiao sections two-sample Kolmogorov–Smirnov (K-S) test on the Ordovician–Devonian samples. Note that 12SC05-3,4,5 is the Shuangming mid- to late-orogenic group; 12SC05-6,7 the Shuangming post-orogenic group; and 11QZ-1,3,5,6,7,8 the Xinqiao mid- to late-orogenic group.*

D value / P value	12SC05-3,4,5	12SC05-6,7	11QZ-1,3,5,6,7,8
12SC05-3,4,5	–	0.405	0.154
12SC05-6,7	0.000	–	0.445
11QZ-1,3,5,6,7,8	0.002	0.000	–

dominant *c.* 830 Ma age peak; and (2) the late-orogenic group (early Silurian) that features a predominant *c.* 850 Ma age peak with increasing Palaeozoic populations, although the older basement signature is not as prominent as same-aged samples from the Shuangming section (Fig. 5h).

To determine whether these groups of samples had any provenance connections, we performed the Kolmogorov–Smirnov (K-S) test (Kolmogorov, 1933; Smirnov, 1944), in which probabilities (*P* values) > 0.05 indicate that the provenance of paired samples cannot be distinguished at a 95 % confidence level (Press *et al.* 1986; Berry *et al.* 2001). The K-S test was first conducted on all paired samples within the sampling section, and then on paired sample groups that were possibly uni-sourced (with *P* values > 0.05 in the first-round test). The first-round results show that the *P* values for all three mid- to late-orogenic sample pairs from the Shuangming section are greater than 0.05, and the paired post-orogenic samples also yielded *P* values of greater than 0.05 (Table 2). However, all the mixing pairs of any mid- to late-orogenic sample with any post-orogenic sample yield *P* values of 0.00 (Table 2). This indicates that all three mid- to late-orogenic samples likely had a common provenance which was statistically different from the sources

shared by the two post-orogenic samples. For the Xinqiao section, all the 15 pairs of mid- and late-orogenic samples yielded *P* values larger than 0.05 (Table 3), implying a common provenance for all six mid- to late-orogenic samples. All the samples were then divided into three groups based on their affinities of possible common provenances, and we ran a second round of the K-S test (Table 4). The results show that all paired sample groups yielded *P* values smaller than 0.05 (Table 4), implying that the provenances of the Shuangming mid- to late-orogenic sediments, the Shuangming post-orogenic sediments and the Xinqiao mid- to late-orogenic sediments are different from each other.

Common provenance for the mid- to late-orogenic samples in the Shuangming section indicates that these detritus were likely transported continuously from similar source region(s) and/or involved recycling of local, older sedimentary rocks. A likely common source region is the northeastern Cathaysia Block (Fig. 1a), where topographic highs above sea level began to be present during Early Ordovician time along the Cathaysia coast (Liu & Xu, 1994; Yao & Li, 2016), and expanded to much of the southeastern Cathaysia Block by Late Ordovician (Fig. 7a) and early Silurian (Fig. 7b) time. As a consequence, older

sedimentary cover sequences (Cambrian and older) and crystalline rocks (the magmatic rocks of age 750–860 Ma and the basement rocks of age 1.77–1.89 Ga; Fig. 7e) were gradually exposed to the surface by erosion (Fig. 7a, b). The large 750–780 Ma zircon population from the interpreted mid-orogenic sample (Fig. 5a) reveals that there were probably abundant mid-Neoproterozoic rift successions and granitic intrusions (Fig. 1b) exposed to the surface during Late Ordovician time (Fig. 7a). The subordinate 920–980 Ma and 630 Ma zircon populations (Fig. 5a) are exotic signatures found in the Ediacaran–Cambrian sedimentary strata in South China (Yao *et al.* 2015), reflecting a contribution of recycled local Ediacaran–Cambrian strata that were uplifted and eroded. The minor 1.77–1.89 Ga zircon population (Fig. 5a) probably suggests either the exposure of a very limited Palaeoproterozoic basement during Late Ordovician time, or the recycling of Palaeoproterozoic zircons from pre-Ordovician sedimentary strata.

By early Silurian time, there are two prominent additions to the detrital age spectra: mid-orogenic (Ordovician) granitic plutons; and Archaean–Palaeoproterozoic ages from the metamorphic basement rocks. The appearance of the prominent 430–450 Ma zircon population in the late-orogenic sandstone samples (Fig. 5b, c) likely reflects the exposure of syn-orogenic plutons, which are widespread in the northeastern Cathaysia Block (Fig. 7b, c, e). The zircon Hf isotopes of these mid- and late-orogenic sediments are similarly distributed and suggest three major new crustal growth events at 0.8 Ga, 1.8 Ga and 2.5 Ga for the source region (Fig. 6), of which the former two episodes were locally supported by the 750–860 Ma bimodal magmatic rocks and 1.77–1.89 Ga crystallized basements, respectively. The 2.5 Ga crustal growth event is yet to be confirmed by Archaean outcrops; it could also be interpreted as imprints from the recycled Ediacaran–Cambrian strata, which are believed by some to have an external source region of northeastern Gondwana (Yu *et al.* 2010; Yao *et al.* 2014, 2015).

The Xinqiao mid- and late-orogenic sandstones (Fig. 5f–h) largely mimic the provenance trend of the Shuangming samples (Fig. 5a–c), with a constant mid-Neoproterozoic age dominance and minor Archean – early Neoproterozoic peaks. Obvious differences between the two datasets are, in the Xinqiao samples: (1) early Palaeozoic populations do not show up in all the late-orogenic samples; (2) pre-1 Ga peaks are not as prominent; and (3) there is the presence of a more distinct 830–860 Ma zircon cluster (Fig. 5). Such differences likely reflect lateral variation of source region characteristics as well as varying degrees of denudation along the orogen.

The provenance of the Shuangming Upper Devonian sediments is characterized by the dominance of *c.* 440 Ma magmatic detritus (Fig. 5d, e), implying widespread exposure of syn-orogenic granites by that time (Fig. 7d, e). The negative Hf values of these *c.* 440 Ma

zircons suggest that the eroded granitic plutons in the northern segment of the Wuyi-Yunkai orogen likely involved little mantle-derived materials (Fig. 6).

6.c. Topographic evolution of the northeastern segment of the Wuyi-Yunkai orogen

The Wuyi-Yunkai orogeny in South China is widely recognized as an intraplate orogeny (e.g. Li, 1998; Li *et al.* 2010; Wang *et al.* 2010), possibly resulted from the far-field stress of the collision between South China and Indian Gondwana (Yao *et al.* 2014). With a lifespan of *c.* 80 Ma (from no later than Early Ordovician – late Silurian time), the orogeny produced the evolving Wuyi-Yunkai orogen and Nanhua foreland basin (Yao & Li, 2016). By late Silurian time, when the orogeny ceased, the Wuyi-Yunkai orogen covered most of the Cathaysia Block and a portion of the southeastern Yangtze Block. The depocentre of the Nanhua foreland basin migrated northwestwards during the orogeny, with the remnant, SW–NE-elongated foreland basin sitting along the southeastern Yangtze Block at the end of the orogeny (Fig. 1a). Whereas the bulk of the Wuyi-Yunkai orogen propagated to the NW by hundreds of kilometres during the orogenic event, the northeastern segment of the orogen did not propagate far into the hinterland (Fig. 1a) as evidenced by the lack of any deformation in regions NW of the Lizhu-Changshan thrust fault in the study region (Figs 1a, 2). Provenance analysis suggests that, during the mid- to late-orogenic stage, the foreland basin in northeastern South China was dominantly fed by detritus eroded from the uplifted Cathaysia coast zone of recycled Ediacaran–Cambrian sedimentary strata and middle Neoproterozoic rift-related volcanoclastic and magmatic rocks, with increasing contributions from the Cathaysia basement rocks and newly exposed mid- to late-orogenic granitic intrusions with time. After the Wuyi-Yunkai orogeny ceased to operate, much of the South China Block underwent a peneplanation process with mid- to late-orogenic granitic plutons widely exposed in the orogen, providing the predominant detrital source for post-orogenic successions. The contrasting Devonian stratigraphic records across the Lizhu-Changshan fault (Fig. 3) indicate that, during Late Devonian time, the Wuyi-Yunkai foreland fold-and-thrust belt SE of the Lizhu-Changshan fault was still on a residual palaeotopographic high above the sea level, therefore not receiving post-orogenic depositional cover until early Carboniferous time (Figs 3, 7d). However, by late Carboniferous time, the entire region of South China was covered by carbonate platform deposits (Liu & Xu, 1994).

7. Conclusions

We analysed the contrasting tectonostratigraphic records across the Lizhu-Changshan fault in eastern South China and documented how the region to the SE of the fault was the foreland fold-and-thrust belt

of the early Palaeozoic Wuyi-Yunkai orogen, whereas the region to the NW of the fault was a remnant foreland basin at the end of the orogenic event which experienced no early Palaeozoic deformation. The Lizhu-Changshan thrust fault therefore defines the northwestern margin of the northeastern segment of the Wuyi-Yunkai orogen. Regional sedimentary facies analysis further indicates that the Wuyi-Yunkai orogen in this region remained a topographic high during Devonian time, but the entire region was covered by carbonate platform deposition by early Carboniferous time, *c.* 60 Myr after the end of the orogenic event.

Provenance analysis of syn-orogenic sandstones from the remnant foreland basin reveals that, during the orogeny, there was a general increase of basement input and contributions from increasingly more widely exposed syn-orogenic granitic intrusions, although lateral variations are also obvious. Detritus for post-orogenic sandstones were dominantly supplied by the erosion of syn-orogenic plutons from the nearby residual topographic highs SE of the Lizhu-Changshan fault.

Declaration of interest

None.

Supplementary material

To view supplementary material for this article, please visit https://doi.org/10.1017/S0016756817000784

References

AMELIN, Y., LEE, D. C., HALLIDAY, A. N. & PIDGEON, R. T. 1999. Nature of the Earth's earliest crust from hafnium isotopes in single detrital zircons. *Nature* **399**, 252–5.

ANDERSON, T. 2002. Correction of common lead in U-Pb analyses that do not report ^{204}Pb. *Chemical Geology* **192**, 59–79.

BERRY, R. F., JENNER, G. A., MEFFRE, S. & TUBRETT, M. N. 2001. A North American provenance for Neoproterozoic to Cambrian sandstones in Tasmania? *Earth and Planetary Science Letters* **192**, 207–22.

BGMRGD (Bureau of Geology and Mineral Resources of Guangdong Province). 1988. *Regional Geology of the Guangdong Province*. Beijing: Geological Publishing House, 971 pp. (in Chinese with English abstract).

BGMRGX (Bureau of Geology and Mineral Resources of Guangxi Province). 1985. *Regional Geology of the Guangxi Province*. Beijing: Geological Publishing House, 853 pp. (in Chinese with English abstract).

BGMRHN (Bureau of Geology and Mineral Resources of Hunan Province). 1988. *Regional Geology of the Hunan Province*. Beijing: Geological Publishing House, 719 pp. (in Chinese with English abstract).

BGMRJX (Bureau of Geology and Mineral Resources of Jiangxi Province). 1984. *Regional Geology of the Jiangxi Province*. Beijing: Geological Publishing House, 921 pp. (in Chinese with English abstract).

BGMRZJ (Bureau of Geology and Mineral Resources of Zhejiang Province). 1989. *Regional Geology of the Zhejiang Province*. Beijing: Geological Publishing House, 688 pp. (in Chinese with English abstract).

BLICHERT-TOFT, J. & ALBAREDE, F. 1997. The Lu–Hf isotope geochemistry of chondrites and the evolution of the mantle–crust system. *Earth and Planetary Science Letters* **148**, 243–58.

CHARVET, J., SHU, L. S., FAURE, M., CHOULET, F., WANG, B., LU, H. F. & BRETON, N. L. 2010. Structural development of the Lower Paleozoic belt of South China: genesis of an intracontinental orogen. *Journal of Asian Earth Sciences* **39**, 309–30.

DECELLES, P. G. & GILES, K. A. 1996. Foreland basin systems. *Basin Research* **8**, 105–23.

DHUIME, B., HAWKESWORTH, C. & CAWOOD, P. 2011. When continents formed. *Science* **331**, 154–5.

GREENTREE, M. R., LI, Z. X., LI, X. H. & WU, H. 2006. Late Mesoproterozoic to earliest Neoproterozoic basin record of the Sibao orogenesis in western South China and relationship to the assembly of Rodinia. *Precambrian Research* **151**, 79–100.

GRIFFIN, W. L., PEARSON, N. J., BELOUSOVA, E., JACKSON, S. E., ACHTERBERGH, E. V., O'REILLY, S. Y. & SHEE, S. R. 2000. The Hf isotope composition of cratonic mantle: LAM-MC-ICPMS analysis of zircon megacrysts in kimberlites. *Geochimica et Cosmochimica Acta* **64**, 133–47.

HAQ, B. U. & SCHUTTER, S. R. 2008. A chronology of Paleozoic sea-level changes. *Science* **322**, 64–8.

HUANG, J., REN, J., JIANG, C., ZHANG, Z. & QIN, D. 1980. *The geotectonic evolution of China*. Beijing: Science Press, 124 pp. (in Chinese with English abstract).

JACKSON, S. E., PEARSON, N. J., GRIFFIN, W. L. & BELOUSOVA, E. A. 2004. The application of laser ablation-inductively coupled plasma-mass spectrometry to in situ U-Pb zircon geochronology. *Chemical Geology* **211**, 47–69.

KOLMOGOROV, A. N. 1933. Sulla determinazione empirica di una legge di distribuzione. *Giornale dell'Istituto Italiano degli Attuari* **4**, 83–91.

LI, W. X., LI, X. H. & LI, Z. X. 2005. Neoproterozoic bimodal magmatism in the Cathaysia Block of South China and its tectonic significance. *Precambrian Research* **136**, 51–66.

LI, X. H. 1999. U–Pb zircon ages of granites from the southern margin of the Yangtze Block: timing of Neoproterozoic Jinning: Orogeny in SE China and implications for Rodinia Assembly. *Precambrian Research* **97**, 43–57.

LI, X. H., LI, W. X., LI, Z. X., LO, C. H., WANG, J., YE, M. F. & YANG, Y. H. 2009. Amalgamation between the Yangtze and Cathaysia Blocks in South China: constraints from SHRIMP U-Pb zircon ages, geochemistry and Nd–Hf isotopes of the Shuangxiwu volcanic rocks. *Precambrian Research* **174**, 117–28.

Li, X. H., Li, Z. X., Ge, W. C., Zhou, H. W., Li, W. X., Liu, Y. & Wingate, M. T. D. 2003a. Neoproterozoic granitoids in South China: crustal melting above a mantle plume at ca. 825 Ma? *Precambrian Research* **122**, 45–83.

Li, Z. X. 1998. Tectonic history of the major East Asian lithospheric blocks since the mid- Proterozoic – a synthesis. In *Mantle Dynamics and Plate Interactions in East Asia* (ed. M. F. J. Flower), pp. 221–43. Washington, DC: American Geophysical Union, Geodynamics Series, vol. 27.

Li, Z. X., Bogdanova, S. V., Collins, A. S., Davidson, A., Dewaele, B., Ernst, R. E., Fitzsimons, I. C. W., Fuck, R. A., Gladkochub, D. P., Jacobs, J., Karlstrom, K. E., Lu, S., Natapov, L. M., Pease, V., Pisarevsky, S. A., Thrane, K. & Vernikovsky, V. 2008. Assembly, configuration, and break-up history of Rodina: a synthesis. *Precambrian Research* **160**, 179–210.

Li, Z. X., Chen, H. L., Li, X. H. & Zhang, F. Q. 2014. *Tectonics of the South China Block – Interpreting the Rock Record*. Beijing: Science Press, 144 pp.

Li, Z. X., Li, X. H., Kinny, P. D. & Wang, J. 1999. The breakup of Rodinia: did it start with a mantle plume beneath South China? *Earth and Planetary Science Letters* **173**, 171–81.

Li, Z. X., Li, X. H., Kinny, P. D., Wang, J., Zhang, S. & Zhou, H. 2003b. Geochronology of Neoproterozoic syn-rift magmatism in the Yangtze Craton, South China and correlations with other continents: evidence for a mantle superplume that broke up Rodinia. *Precambrian Research* **122**, 85–109.

Li, Z. X., Li, X. H., Wartho, J. A., Clark, C., Li, W. X., Zhang, C. L. & Bao, C. M. 2010. Magmatic and metamorphic events during the early Paleozoic Wuyi-Yunkai orogeny, southeastern South China: new age constraints and pressure–temperature conditions. *Geological Society of America Bulletin* **122**, 772–93.

Li, Z. X., Li, X. H., Zhou, H. & Kinny, P. D. 2002. Grenvillian continental collision in south China: new SHRIMP U-Pb zircon results and implications for the configuration of Rodinia. *Geology* **30**, 163–6.

Liu, B. & Xu, X. 1994. *Atlas of Lithofacies and Paleogeography of South China*. Beijing: Science Press, 188 pp. (in Chinese with English Abstract).

Ludwig, K. R. 2001. Isoplot/Ex version 2.49 – A geochronological toolkit for Microsoft excel. Berkeley Geochronological Centre Special Publication No. 1, 56 pp.

Moores, E. M. & Twiss, R. J. 1995. *Tectonics*. New York: WH Freeman, 415 pp.

Morel, M. L. A., Nebel, O., Nebel-Jacobsen, Y. J., Miller, J. S. & Vroon, P. Z. 2008. Hafnium isotope characterization of the GJ-1 zircon reference material by solution and laser-ablation MC-ICPMS. *Chemical Geology* **255**, 231–35.

Press, W. H., Flannery, B. P., Teukolsky, S. A. & Vetterling, W. T. 1986. *Numerical Recipes: The Art of Scientific Computing*. Cambridge: Cambridge University Press, 186 pp.

Ren, J. 1964. A preliminary study on pre-Devonian geotectonic problems of southeastern China. *Acta Geologica Sinica* **44**, 418–31.

Ren, J. 1991. On the geotectonics of southern China. *Acta Geologica Sinica* **4**, 111–30.

RGMRZJ-a. 1966. *Regional Geological Mapping and Report of Zhejiang Province–1:200,000 Jinhua Sheet*. Beijing: Institute of Geoscience, Ministry of Geology (in Chinese).

RGMRZJ-b. 1970. *Regional Geological Mapping and Report of Zhejiang Province–1:200,000 Quxian Sheet*. Beijing: Institute of Geoscience, Ministry of Geology (in Chinese).

Rong, J. Y., Zhang, R. B., Xu, H. G., Huang, B. & Yu, G. H. 2010. Expansion of the Cathaysian Oldland through the Ordovician-Silurian transition: emerging evidence and possible dynamics. *Science in China (Earth Sciences)* **53**, 1–17.

Shu, L. S., Faure, M., Yu, J. H. & Jahn, B. M. 2011. Geochronological and geochemical features of the Cathaysia block (South China): new evidence for the Neoproterozoic breakup of Rodinia. *Precambrian Research* **187**, 263–76.

Smirnov, N. V. 1944. Approximate laws of distribution of randomvariables from empirical data. *Uspekhi Matematicheskikh Nauk* **10**, 179–206 (in Russian).

Soderlund, U., Patchett, P. J., Vervoort, J. D. & Isachsen, C. E. 2004. The ^{176}Lu decay constant determined by Lu-Hf and U-Pb isotope systematics of Precambrian mafic intrusions. *Earth and Planetary Science Letters* **219**, 311–24.

Van Achterbergh, E., Ryan, C. G., Jackson, S. E. & Griffin, W. L. 2001. Data reduction software for LA-ICP-MS: appendix. In *Laser Ablation-ICP-Mass Spectrometry in the Earth Sciences: Principles and Applications* (ed. P. J. Sylvester), pp. 239–43. Mineralogist Association Canada (MAC), Ottawa, Short Course Series 29.

Wan, Y., Liu, D., Wilde, S. A., Cao, J., Chen, B., Dong, C., Song, B. & Du, L. 2010. Evolution of the Yunkai Terrane, South China: evidence from SHRIMP zircon U-Pb dating, geochemistry and Nd isotope. *Journal of Asian Earth Sciences* **37**, 140–53.

Wang, X. L., Zhou, J. C., Griffin, W. L., Wang, R. C., Qiu, J. S., O'Reilly, S. Y., Xu, X., Liu, X. M. & Zhang, G. L. 2007. Detrital zircon geochronology of Precambrian basement sequences in the Jiangnan orogen: Dating the assembly of the Yangtze and Cathaysia Blocks. *Precambrian Research* **159**, 117–31.

Wang, X. L., Zhou, J. C., Qiu, J. S., Zhang, W. L., Liu, X. M. & Zhang, G. L. 2006. LA-ICP-MS U-Pb zircon geochronology of the Neoproterozoic igneous rocks from Northern Guangxi, South China: implications for tectonic evolution. *Precambrian Research* **145**, 111–30.

Wang, Y., Fan, W., Zhao, G., Ji, S. & Peng, T. 2007. Zircon U-Pb geochronology of gneissic rocks in the Yunkai massif and its implications on the Caledonian event in the South China Block. *Gondwana Research* **12**, 404–16.

Wang, Y., Zhang, A., Fan, W., Zhang, Y. & Zhang, Y. 2013. Origin of paleosubduction-modified mantle for Silurian gabbro in the Cathaysia Block: Geochronological and geochemical evidence. *Lithos* **160–1**, 37–54.

Wang, Y., Zhang, F., Fan, W., Zhang, G., Chen, S., Cawood, P. A. & Zhang, A. 2010. Tectonic setting of the South China Block in the early Paleozoic: resolving intracontinental and ocean closure models from detrital zircon U-Pb geochronology. *Tectonics* **29**, https://doi.org/10.1029/2010TC002750.

Wiedenbeck, M., Alle, P., Corfu, F., Griffin, W. L., Meer, M., Oberli, F., Vonquadt, A., Roddick, J. C. & Spegel, W. 1995. Three natural zircon standards for U–Th–Pb, Lu–Hf, trace element and REE analysis. *Geostandards and Geoanalytical Research* **19**, 1–23.

WIEDENBECK, M., HANCHAR, J. M., PECK, W. H., SYLVESTER, P., VALLEY, J., WHITEHOUSE, M., KRONZ, A., MORISHITA, Y., NASDALA, L., FIEBIG, J., FRANCHI, I., GIRARD, J. P., GREENWOOD, R. C., HINTON, R., KITA, N., MASON, P. R. D., NORMAN, M., OGASAWARA, M., PICCOLI, P. M., RHEDE, D., SATOH, H., SCHULZ-DOBRICK, B., SPICUZZA, M. J., TERADA, K., TINDLE, A., TOGASHI, S., VENNEMANN, T., XIE, Q. & ZHENG, Y. F. 2004. Further characterisation of the 91500 zircon crystal. *Geostandards Newsletter* **28**, 9–39.

WU, F. Y., YANG, Y. H., XIE, L. W., YANG, J. H. & XU, P. 2006. Hf isotopic compositions of the standard zircons and baddeleyites used in U-Pb geochronology. *Chemical Geology* **234**, 105–26.

WU, R. X., ZHENG, Y. F., WU, Y. B., ZHAO, Z. F., ZHANG, S. B., LIU, X. & WU, F. Y. 2006. Reworking of juvenile crust: Element and isotope evidence from Neoproterozoic granodiorite in South China. *Precambrian Research* **146**, 179–212.

XIE, L. W., ZHANG, Y. B., ZHANG, H. H., SUN, J. F. & WU, F. W. 2008. In situ simultaneous determination of trace elements, U-Pb and Lu–Hf isotopes in zircon and baddeleyite. *Chinese Science Bulletin* **53**, 1565–73.

XU, Y., DU, Y., CAWOOD, P. A., ZHU, Y., LI, W. & YU, W. 2012. Detrital zircon provenance of Upper Ordovician and Silurian strata in the northeastern Yangtze Block: response to orogenesis in South China. *Sedimentary Geology* **267–8**, 63–72.

YANG, Z., CHENG, Y. Q. & WANG, H. C. 1986. *The Geology of China*. Oxford: Clarendon Press, 276 pp.

YAO, W. H. & LI, Z. X. 2016. Tectonostratigraphic history of the Ediacaran–Silurian Nanhua foreland basin in South China. *Tectonophysics* **674**, 31–51.

YAO, W. H., LI, Z. X., LI, W. X., LI, X. H. & YANG, J. H. 2014. From Rodinia to Gondwanaland: a tale of detrital zircon provenance analyses from the southern Nanhua Basin, South China. *American Journal of Science* **314**, 278–313.

YAO, W. H., LI, Z. X., LI, W. X., SU, L. & YANG, J. H. 2015. Detrital provenance evolution of the Ediacaran–Silurian Nanhua foreland basin, South China. *Gondwana Research* **28**, 1449–65.

YAO, W. H., LI, Z. X., LI, W. X., WANG, X. C., LI, X. H. & YANG, J. H. 2012. Post-kinematic lithospheric delamination of the Wuyi-Yunkai orogen in South China: evidence from ca. 435 Ma high-Mg basalts. *Lithos* **154**, 115–29.

YU, J. H., O'REILLY, S. Y., WANG, L., GRIFFIN, W. L., ZHANG, M., WANG, R., JIANG, S. & SHU, L. 2008. Where was South China in the Rodinia supercontinent? Evidence from U-Pb geochronology and Hf isotopes of detrital zircons. *Precambrian Research* **164**, 1–15.

YU, J. H., O'REILLY, S. Y., WANG, L., GRIFFIN, W. L., ZHOU, M. F., ZHANG, M. & SHU, L. 2010. Components and episodic growth of Precambrian crust in the Cathaysia Block, South China: Evidence from U-Pb ages and Hf isotopes of zircons in Neoproterozoic sediments. *Precambrian Research* **181**, 97–114.

YU, Y., HUANG, X. L., HE, P. L. & LI, J. 2016. I-type granitoids associated with the early Paleozoic intracontinental orogenic collapse along pre-existing block boundary in South China. *Lithos* **248–51**, 353–65.

ZHAO, G. & CAWOOD, P. A. 1999. Tectonothermal evolution of the Mayuan assemblage in the Cathaysia Block: implications for Neoproterozoic collision-related assembly of the South China Craton. *American Journal of Science* **299**, 309–39.

ZHOU, M. F., MA, Y., YAN, D. P., XIA, X., ZHAO, J. H. & SUN, M. 2006. The Yanbian Terrane (Southern Sichuan Province, SW China): a Neoproterozoic arc assemblage in the western margin of the Yangtze Block. *Precambrian Research* **144**, 19–38.

ZHOU, M. F., YAN, D. P., KENNEDY, A. K., LI, Y. & DING, J. 2002. SHRIMP U-Pb zircon geochronological and geochemical evidence for Neoproterozoic arc-magmatism along the western margin of the Yangtze Block, South China. *Earth and Planetary Science Letters* **196**, 51–67.